AFRL-PR-WP-TP-2006-206

EFFECT OF O_2 PARTIAL PRESSURE ON $YBa_2Cu_3O_{7-\delta}$ THIN FILM GROWTH BY PULSED LASER DEPOSITION

T.J. Haugan, P.N. Barnes, L. Brunke, I. Maartense, and J. Murphy

APRIL 2004

Approved for public release; distribution is unlimited.

STINFO COPY

PROPULSION DIRECTORATE
AIR FORCE MATERIEL COMMAND
AIR FORCE RESEARCH LABORATORY
WRIGHT-PATTERSON AIR FORCE BASE, OH 45433-7251

REPORT DOCUMENTATION PAGE

Form Approved
OMB No. 0704-0188

1. REPORT DATE *(DD-MM-YY)*	2. REPORT TYPE	3. DATES COVERED *(From - To)*
April 2006	Journal Article Postprint	02/01/2002 – 02/01/2003

4. TITLE AND SUBTITLE
EFFECT OF O_2 PARTIAL PRESSURE ON $YBa_2Cu_3O_{7-\delta}$ THIN FILM GROWTH BY PULSED LASER DEPOSITION

5a. CONTRACT NUMBER
In-house

5b. GRANT NUMBER

5c. PROGRAM ELEMENT NUMBER
61102F/62203F

6. AUTHOR(S)
T.J. Haugan, P.N. Barnes, I. Maartense, L. Brunke, and J. Murphy (AFRL/PRPG)
T. Haugan (UES, Inc.)

5d. PROJECT NUMBER
3145

5e. TASK NUMBER
32

5f. WORK UNIT NUMBER
31453279

7. PERFORMING ORGANIZATION NAME(S) AND ADDRESS(ES)

Power Generation Branch (AFRL/PRPG)
Power Division
Propulsion Directorate
Air Force Research Laboratory, Air Force Materiel Command
Wright-Patterson Air Force Base, OH 45433-7251

UES, Inc.

8. PERFORMING ORGANIZATION REPORT NUMBER
AFRL-PR-WP-TP-2006-206

9. SPONSORING/MONITORING AGENCY NAME(S) AND ADDRESS(ES)

Propulsion Directorate
Air Force Research Laboratory
Air Force Materiel Command
Wright-Patterson AFB, OH 45433-7251

10. SPONSORING/MONITORING AGENCY ACRONYM(S)
AFRL-PR-WP

11. SPONSORING/MONITORING AGENCY REPORT NUMBER(S)
AFRL-PR-WP-TP-2006-206

12. DISTRIBUTION/AVAILABILITY STATEMENT
Approved for public release; distribution is unlimited.

13. SUPPLEMENTARY NOTES
Journal article published in *Physica C*, Issue 397 (2003), published by Elsevier B.V.

PAO case number: AFRL/ASC 02-0247; Date cleared: 25 Feb 2002. Paper contains color.

14. ABSTRACT
$YBa_2Cu_3O_{7-\delta}$ thin films were processed by pulsed laser deposition on (1 0 0) LaAlO3 substrates using O_2 partial pressures from 120 to 1200 mTorr. The effect of O_2 pressure on film properties including room temperature resistivities and microstructures was studied for a unique set of deposition parameters. The film quality was observed to remain high over a wide range of O2 partial pressures, with much less sensitivity to O_2 pressure than previous studies which are compared. For O_2 pressures from 200 to 1200 mTorr, superconducting transition temperatures consistently reached values >91.5 K and transport critical current densities were 3–5 MA/cm^2 (77 K, self-field).It is proposed that less sensitivity of film properties to O_2 pressure is achieved by: (1) reducing the particle velocity of the plume below a critical threshold, and (2) using a deposition temperature of 785 °C for adequate surface activation.

15. SUBJECT TERMS
$YBa_2Cu_3O_{7-\delta}$, oxygen pressure, pulsed laser deposition, HTS thin films

16. SECURITY CLASSIFICATION OF:			17. LIMITATION OF ABSTRACT:	18. NUMBER OF PAGES	19a. NAME OF RESPONSIBLE PERSON (Monitor)
a. REPORT	b. ABSTRACT	c. THIS PAGE			Paul N. Barnes
Unclassified	Unclassified	Unclassified	SAR	18	19b. TELEPHONE NUMBER *(Include Area Code)* N/A

Available online at www.sciencedirect.com
SCIENCE DIRECT®
Physica C 397 (2003) 47–57
PHYSICA C
www.elsevier.com/locate/physc

Effect of O_2 partial pressure on $YBa_2Cu_3O_{7-\delta}$ thin film growth by pulsed laser deposition

T. Haugan *, P.N. Barnes, L. Brunke, I. Maartense, J. Murphy

Air Force Research Laboratory, 2645 Fifth St. Ste. 13, Wright-Patterson AFB, OH 45433-7919, USA

Received 1 February 2003; received in revised form 24 April 2003; accepted 24 April 2003

Abstract

$YBa_2Cu_3O_{7-\delta}$ thin films were processed by pulsed laser deposition on (1 0 0) $LaAlO_3$ substrates using O_2 partial pressures from 120 to 1200 mTorr. The effect of O_2 pressure on film properties including room temperature resistivities and microstructures was studied for a unique set of deposition parameters. The film quality was observed to remain high over a wide range of O_2 partial pressures, with much less sensitivity to O_2 pressure than previous studies which are compared. For O_2 pressures from 200 to 1200 mTorr, superconducting transition temperatures consistently reached values >91.5 K and transport critical current densities were 3–5 MA/cm^2 (77 K, self-field). It is proposed that less sensitivity of film properties to O_2 pressure is achieved by: (1) reducing the particle velocity of the plume below a critical threshold, and (2) using a deposition temperature of 785 °C for adequate surface activation.

PACS: 74.76.B; 74.72.B; 81.15.F
Keywords: $YBa_2Cu_3O_{7-\delta}$; Oxygen pressure; Pulsed laser deposition; HTS thin films

1. Introduction

The growth of $YBa_2Cu_3O_{7-\delta}$ (YBCO) thin films is of great interest for superconducting applications such as AC wires, generators, or motors operating at 77 K, because of the excellent critical current densities (J_c) and intrinsic pinning properties of YBCO in magnetic fields [1]. Recently, the development of coated conductor wire technologies for aligning YBCO grains on metallic substrates with $J_c > 1$ MA/cm^2 has stimulated further interest in understanding and improving YBCO thin film deposition techniques [2–4]. One of these techniques of interest for coated conductor development is pulsed laser deposition [5]. While the studies herein were performed on $LaAlO_3$ single crystals, the lattice mismatch and other properties of $LaAlO_3$ are similar to buffer layer materials such as CeO_2 used as final buffer layers on biaxially textured metallic substrates. Therefore it is expected that the work herein can also be applied for coated conductors, as well as work that requires deposition on single crystal substrates.

* Corresponding author. Tel.: +1-937-255-6940; fax: +1-937-656-4095.
E-mail address: timothy.haugan@wpafb.af.mil (T. Haugan).

0921-4534/$ - see front matter
doi:10.1016/S0921-4534(03)01088-8

Pulsed laser deposition (PLD) is a well-known method for depositing YBCO thin films with generally excellent properties. Although PLD of YBCO has been studied extensively, there are many factors that are yet unknown. The parameter space for PLD includes many variables such as substrate temperature, O_2 pressure during deposition, target-to-substrate distance; laser properties including fluence, wavelength, beam profile uniformity and repetition rate; target properties including density and optical absorption; ablation footprint size and dimensions (which affect plume shape); and substrate parameters such as chemical composition and lattice constant matches. These parameters are interrelated and optimization for one parameter can involve a range of optimization for others.

The role of oxygen pressure in pulsed laser deposition of YBCO was studied early on after the introduction of the high temperature superconductors, and has received renewed attention recently with the development of the coated conductor technology [5–14]. In addition to affecting parameters discussed above, varying the oxygen deposition pressure during PLD can influence film growth by changing the ionic ratios of the plume [5,6], altering the chemical species during deposition [5], and varying the crystallization temperature of the deposited compound. Up to 1994, O_2 pressures were typically studied from about 50 to 400 mTorr, and the best deposition conditions were achieved within this range [5,7]. Recently, however, there is increasing evidence that excellent properties can be achieved at higher O_2 pressures of 100–800 mTorr [8–11]. However in studies thus far, a narrow window of O_2 pressure existed where an optimal T_c and J_c could be obtained [7–11].

This work extends the study of O_2 deposition pressures ranging from 120 to 1200 mTorr, and results are compared to previous studies on effects of O_2 pressure. Previously, all data supported the supposition that a narrow window of O_2 pressure was required to achieve optimal film quality [7–14], and both microstructural and transition data indicated good film quality could only be obtained with the plume just touching the substrate [12–14]. To model the dependence on O_2 pressure, it was observed that at lower substrate temperature, a relation between target-to-substrate distance (D) and O_2 pressure (P) existed with $PD^{5(1-n)} = \text{const} \sim$ particle velocity, and n is a constant in the range of 0.4–0.6 that fits the experimental P–D data [7]. For any value of D chosen, a very narrow range of O_2 pressure was required to maintain a constant velocity of particle bombardment. The particle bombardment presumably increased the surface activation and enabled film growth at lower temperatures [7]. The results in this paper at higher substrate temperature, however, provide substantial evidence that cannot be explained with this model, and indicates that different mechanisms must be considered for film growth. Herein, both microstructural and transport properties were optimized in a very wide range of pressure (200–1200 mTorr). With the plume length (L_p) extending to touch the substrate only at 600 mTorr, optimum results were obtained with the substrate located both inside and outside of the plume; $D/L_p \sim 0.7$–1.2. These results are explained as a consequence of several film growth mechanisms.

2. Experimental

Parameters used for pulsed laser deposition are described in Table 1. The YBCO powder in the target was prepared by chemical precipitation with submicron size (nominally 99.999% pure) [15]. Films were deposited in a spherical-shaped vacuum chamber (~20 cm diameter) with a 5 cm diameter substrate heater [16]. The temperature of the heater block is reported herein, measured with K-type thermocouples placed in contact with the heater block directly behind where the samples were mounted. The standard measurement error for K-type thermocouples is 0.75% for temperatures >300 °C (Omega Engineering Inc., Stamford, CT). An excimer laser (Lambda Physik, model LPX 305i) operating at the KrF wavelength was used. $LaAlO_3$ single crystal substrates were provided by the manufacturer epitaxially polished on both sides, and were attached to the heater using a thin layer of colloidal Ag paint. The oxygen deposition pressure was measured with capacitance

Table 1
Pulsed laser deposition parameters for work herein and other studies

	This work	Ref. [7]	Ref. [8]	Ref. [9]	Ref. [10]	Ref. [11]
Laser wavelength (nm)	248	193	248	308	248	308
Laser pulsewidth (ns)	25	15	25	30	25	25
Pulse energy (mJ)	200	–	45	93	104	103
Ablation spot size (mm^2)	$\sim 1 \times 6.3$	–	$\sim 1 \times 4.5$	5.45	$\sim 2 \times 4$	5
Laser fluence (J/cm^2)	3.2	3	1	1.7	1.3	2.1
Repetition rate (Hz)	4	–	5	4	10	10
Target-to-substrate distance (cm)	6	6	6	4.5	6.5	3.5
Laser strike angle (° from target normal)	45	–	–	–	45	45
Target density (%)	92	–	–	85	High	75
Substrate	$LaAlO_3$	MgO	$LaAlO_3$, MgO	$SrTiO_3$, MgO	$LaAlO_3$	$SrTiO_3$
Substrate size (mm^3)	12×3.2–5×0.5	–	10×10	–	15×15	$\sim 1.3 \times 1.3$
Substrate temperature (°C)	785	680	780 $LaAlO_3$, 800 MgO	750	770	725
Film thickness (μm)	0.2–0.8	–	0.1–0.2	–	~0.3	–
O_2 in situ anneal	500 °C, 760 Torr	–	550 °C, flowing O_2	–	470 °C, 600 Torr	700 °C, 760 Torr

manometer and convectron gauges with <1% variation. Oxygen gas (99.999% purity) flowed into the chamber during growth at ~1 l/min, and the oxygen pressure in the chamber was kept constant in the chamber using a downstream throttle-valve control on the pumping line. The YBCO target was resurfaced periodically with SiC sandpaper, and conditioned with ~3000 laser pulses using a laser fluence of 2–4 J/cm^2 prior to deposition. The target rotated during deposition and the laser beam was scanned across 1.5 cm of the 5 cm diameter target. Scanning the target allowed more uniform wear of the target and provided a larger area of deposition. The plume varied only slightly as a consequence of scanning. The $LaAlO_3$ (1 0 0) single crystal substrates were ultrasonically cleaned for 2 min each using first acetone, followed by dehydrated ethyl alcohol.

The background pressure in the chamber was reduced to $<10^{-6}$ Torr prior to depositions. Samples were heated from room temperature to deposition temperature of 785 °C at 1270 °C/h. Film thickness was controlled by varying the deposition time. After deposition, films were cooled from 785 to 750 °C at 1270 °C/h before turning off the vacuum pumps and O_2 pressure control. Subsequently the O_2 flow was increased to ~1.5 l/min into the chamber. The films were then cooled from 750 °C to 500 °C at a rate of 1270 °C/h, and held at 500 °C for 30 min, during which the O_2 pressure reached 1 atm. The films were cooled from 500 °C to 250 °C at about 1250 °C/h, and from 250 °C to room temperature using the natural cooling rate of the heater block (~800 °C/h).

After deposition, current and voltage contacts were patterned onto the films by DC magnetron sputter deposition of Ag with ~3 μm thickness. The current contacts covered the sample ends (~2 mm on each end), and the voltage contacts were separated from the current contact, with a size of ~2 mm^2 and centered about 0.5 cm apart. The resistance of the Ag contacts was reduced by annealing in pure O_2 at 550 °C for 30 min with heating and cooling rates of 200 °C/h [17]. The non-Ag coated areas of the films were patterned to make macrobridges 0.3 cm long and 0.048 cm wide, using 248 nm KrF laser etching through a precisely machined Al_2O_3 mask. The laser parameters for etching were fluence of 0.1–0.2 J/cm^2, 1–2 Hz repetition rate, and number of pulses 100–1000 depending on film thickness.

Transport critical current density (J_c) measurements were made in liquid nitrogen at 77.2 K with the 4-pt probe method (self-field) using pogo

pins for current contacts [17,18], and a 1 μv/cm criterion. The temperature of liquid N_2 was measured with a Lakeshore 340 Temperature Controller and different Cernox™ RTD sensors calibrated by the manufacturer using NIST traceable standards. Current was applied to the sample by a step-ramp method: a current step interval of 0.2–0.5 s, a ramp rate of 0.25–1.0 A/s, and a voltage sample period 2–4 times smaller than the current step interval. The maximum current step size was 0.2 A. Measurements of J_c were repeatable for these ranges of step-ramp parameters. Current and voltage sources for resistivity and critical current measurements were calibrated on a regular basis. The film thickness was measured with a Tencor P10 stylus profilometer in areas of the $LaAlO_3$ substrates free of microcrystalline undulations, and with SEM on fractured cross-sections. The thickness of every sample was measured in areas near/or on the bridge areas across step-edges created by etching with ~4% volume fraction HNO_3 acid. Acid etching had no measurable effect on the $LaAlO_3$ substrates, however, was able to quickly etch the film in only about 10 s. For room temperature resistivity measurements, care was used to remove all excess film and Ag paint on the sample sides and bottom with sandpaper or dilute HCl etch.

The superconducting transition temperature (T_c) was measured using an AC susceptibility technique with the amplitude of the magnetic sensing field, h, varied from 0.025 to 2.2 Oe, at a frequency of approximately 4 kHz [19,20]. Note that the AC susceptibility technique provides information about primary and secondary transitions of the entire film, rather than a defined path that is obtained with transport T_c measurements. Transition widths and peak shifts of the loss coefficient (χ'') for varying h can give a qualitative measure of the intergrain coupling and J_c [19,20]. The AC susceptibility technique has the advantage of measuring T_cs of films non-destructively as deposited without any effect from Ag metallization or etching. Herein, T_cs were measured immediately after film deposition and prior to adding Ag contacts.

For T_c measurements, samples were mounted onto the end of a sapphire rod with a GaAlAs temperature sensor embedded in the rod. The sapphire rod was held in a cryogenic dewar filled with gaseous He evaporated from the liquid. Samples were measured as the He gas was warmed from 4.2 K. The warming rate in the transition region was very slow at ~0.06 K/min, which provided a stable and reproducible measurement. The T_c transition was measured at 0.03 K increments. The GaAlAs temperature sensor was accurate within $\leqslant$0.1 K at three calibration points: liquid He at 4.2 K, liquid N_2 at 77.2 K, and room temperature.

3. Results

The effect of varying O_2 deposition pressure on plume characteristics is shown in Fig. 1. As the O_2 pressure was increased, the plume reduced in width and length as expected from increased collisional dampening [5]. The visible part of the plume just reached the substrate at an O_2 pressure of 600 mTorr. For a lower deposition pressure (120–200 mTorr), the plume was quite broad and deposited the target material over a cross-sectional area of about 6 cm diameter. The plumes were approximately spherical shaped (width/length $\sim$ 0.9), and uniform and soft around the edges. The spherical-shaped plume is in contrast with most previous reports with more forward-directed plumes [5,12,13]. Fig. 1 also shows a transition from yellowish to reddish color in the outer edge of the plume, as the oxygen pressure was increased. This visible red emission corresponds to increased formation of YO [6].

As the O_2 chamber pressure was varied, the deposition rate was changed as shown in Fig. 2. The trend of higher deposition rate when the plume edge touches the substrate is consistent with previous work [10]. For O_2 pressure $<$ 600 mTorr, the plume impinged on the substrate, which may increase the possibility for re-sputtering resulting from bombardment of high energy particles in the plume. For O_2 pressure $>$ 600 mTorr, the plume is more focused which increases the localized deposition.

A plot of the superconducting transition of a representative film with $T_c \sim 92$ K is given in

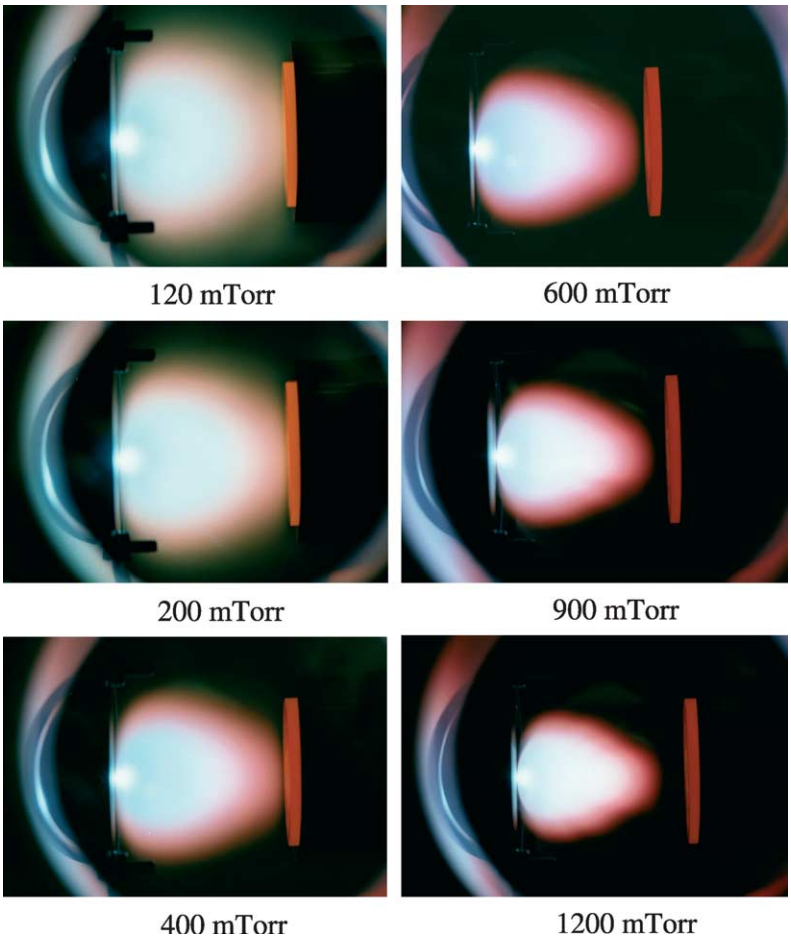

Fig. 1. Photographic images of YBCO plume formation as a function of O_2 deposition pressure. The heater block (5 cm diameter) is seen to the right of the plume glowing red at 785 °C. The long side of the rectangular footprint of the laser was positioned perpendicular to the plane of the photographs.

Fig. 3. The onset of the transition is quite high at 92.0 K, reaching nearly the maximum for the $YBa_2Cu_3O_{7-\delta}$ compound of 92.6 K [21]. For 0.025 Oe applied AC field, the FWHM width of the χ'' peak was <0.2 K. The shift of the χ'' peak maximum as h was varied from 0.025 to 2.2 was ~0.9 K. Similar shifts of the χ'' peak as small as 0.65 K were observed for films with $T_c > 91.5$ K. Such narrow transitions and peak shifts as measured by AC susceptibility generally indicate the film has excellent uniformity and intergrain coupling and a high transport J_c (>1 MA/cm^2 at 77 K) [19,20].

Fig. 4 plots the T_c onset for films deposited with varying O_2 pressure, and compares the results with T_cs from previous studies measured by both AC susceptibility and transport currents [7–11]. The comparison of T_cs measured by different methods is meaningful, as T_cs measured by AC susceptibility usually correspond to within 1 K to the zero-resistance point of a transport measurement [10]. The T_cs in Fig. 4 showed a gradual increase from ~88 to >91.5 K as the O_2 pressure was increased from 120 to 400 mTorr. For O_2 pressure from 400 to 1200 mTorr, the T_cs were very high and consistent at 91.8 ± 0.4 K for multiple deposition runs

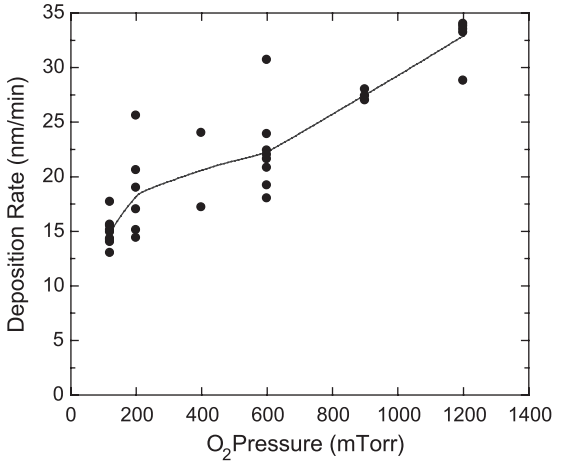

Fig. 2. Deposition rate of YBCO films on $LaAlO_3$ substrates for varying O_2 deposition pressure.

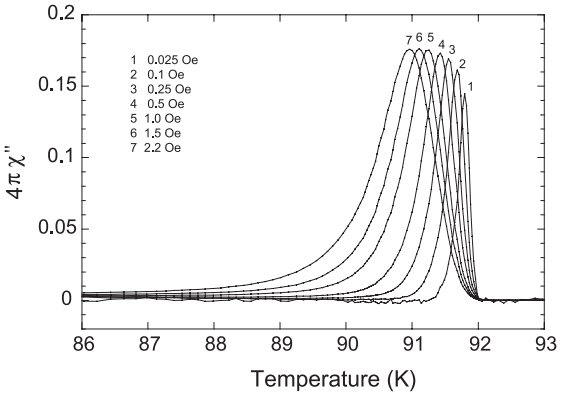

Fig. 3. Superconducting transition of a film deposited at O_2 pressure of 1200 mTorr, as measured by AC susceptibility for different magnetic sensing fields.

and for all samples in these runs without exception. Typically, high T_cs of ~90–91 K are usually reported for YBCO thin films, regardless of the deposition method [5].

The trend in Fig. 4 of constant T_c for a wide range of O_2 pressures from 400 to 1200 mTorr varies from other studies where maximum T_c was obtained for narrower windows of O_2 pressure [7–11]. The variation of results in Fig. 4 indicates the potentially subtle effect of different growth conditions (Table 1) on T_c and film properties. The most distinctly different result presented in Fig. 4 was

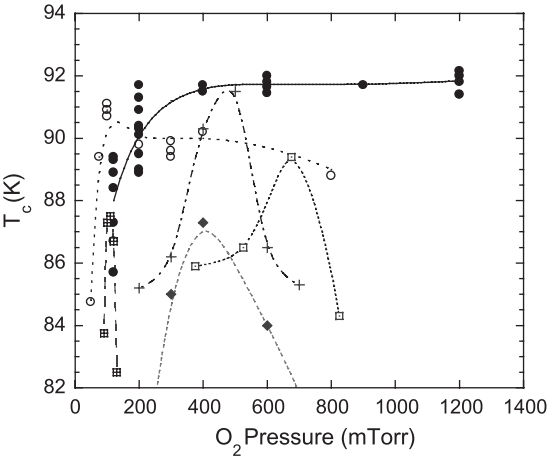

Fig. 4. T_c onset of YBCO films as a function of O_2 deposition pressure for 0.2–0.8 μm thick films (●). T_cs for 600 and 1200 mTorr were from four deposition runs at each pressure. T_cs from previous studies are included for comparison: (⊞) [7]; (+) [8]; (⊡) [9]; (○) [10] and (◆) [11]. T_cs from previous studies were measured by the resistive method [7,8], by AC susceptibility [9,10], and by an unspecified method [11]. Lines are guides to the eye.

from a study in which a low growth temperature of 680 °C was chosen along with MgO as a substrate [7]. Another study found only small differences between MgO and $LaAlO_3$ for growth at 700–840 °C [8]. Therefore, the lower growth temperature of 680 °C combined with a highly energetic plume might presumably be the dominant factors for reducing the sensitivity to O_2 pressure for Ref. [7].

Results in Fig. 4 can be compared to T_cs of films quenched from the deposition temperature for varying O_2 pressure [14]. In [14], T_c was found to depend on whether the film was located inside or outside the plume, and higher T_cs were measured for films deposited at or beyond the plume edge. From Fig. 4, T_c is consistently 91.8 ± 0.4 K for films located both inside and outside the plume. Therefore, assuming the physical mechanisms are similar for the work herein, the T_cs in Fig. 4 may partially be a consequence of the post-deposition treatment and cooling in an O_2 atmosphere, although this is not conclusive.

Fig. 5 plots transport J_c by the four-probe method as a function of O_2 deposition pressure, and compares it to results from a similar study

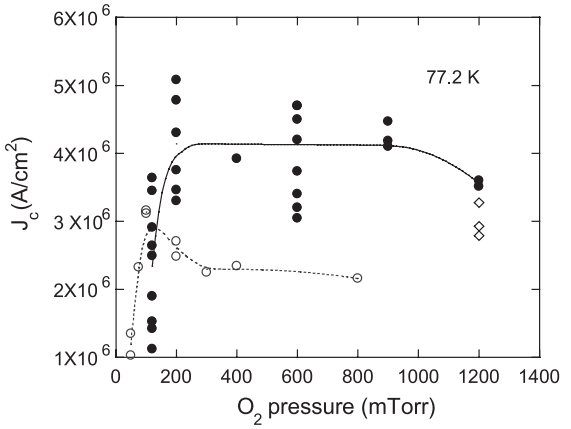

Fig. 5. Transport J_c of 0.2–0.6 μm thick YBCO films measured in liquid nitrogen as a function of O_2 deposition pressure (●) including values for fluence = 4.5 J/cm^2 (◇), and (○) from Ref. [10] using their estimated extrapolation from magnetic measurements. J_cs at 200 and 600 mTorr were from three or more deposition runs at each pressure. Lines are guides to the eye.

[10]. For O_2 pressure from 200 to 1200 mTorr, J_cs were consistently at 3–5 MA/cm^2 as measured at 77.2 K in self-field. The spread of J_cs in Fig. 5 for a given O_2 pressure results mostly from the dependence of J_c on film thickness, as given in Fig. 6 for films deposited for different O_2 pressures ranges.

As seen in Fig. 5, transport J_c had a slightly different dependence on O_2 pressure than T_c. For example, at 200 mTorr J_cs were high, whereas T_cs were in the range of 89–92 K. When the substrates were located outside of the plume for O_2 pressure >900 mTorr, J_cs showed a slight decrease to about 3 MA/cm^2, even though the T_cs were consistently near 92 K. The decrease in J_c for O_2 pressure ⩾900 mTorr might be correlated with increasing surface roughness, as films deposited at these pressures appeared grayish to the eye, and the surfaces as viewed by SEM contained high densities of micron-size particulates (also shown later in this paper).

The effect of O_2 deposition pressure on the room temperature resistivity (ρ) of films represented in Fig. 5 is given in Fig. 7. The resistivity had a different dependence on O_2 pressure than T_c or J_c, with the lowest values of resistivity obtained at O_2 pressure about 200–400 mTorr. The change in resistivity in Fig. 7 is not related to the J_cs in Fig. 5, as there was only a small correlation of resistivity with J_c, as shown in Fig. 8. In Fig. 8, higher J_cs were slightly correlated with higher room temperature resistivity, although the relationship was not very strong.

The microstructures of films deposited at different O_2 pressures are shown in Fig. 9. Films deposited at 120 mTorr had a high concentration of pinhole defects which may have been caused by selective resputtering from the very high translational kinetic energy particles in the plume (up to 50 eV) [22], or reduced ripening of island growth at lower deposition rates [5]. Films deposited at

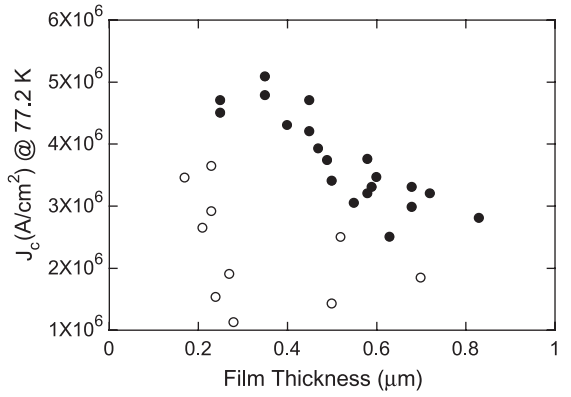

Fig. 6. The effect of film thickness on J_c for films deposited at 120 mTorr (○) and 200–600 mTorr (●).

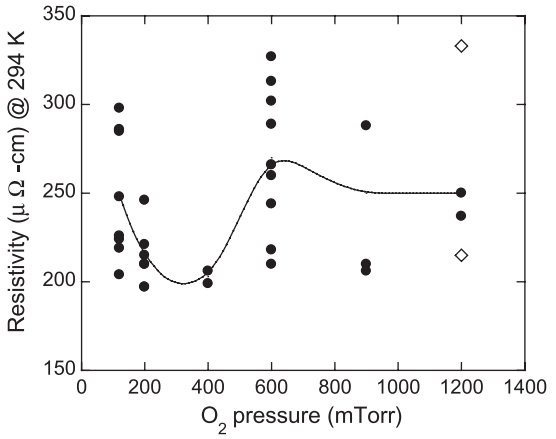

Fig. 7. Room temperature resistivity of YBCO films as a function of O_2 deposition pressure, including values for fluence = 4.5 J/cm^2 (◇). Lines are guides to the eye.

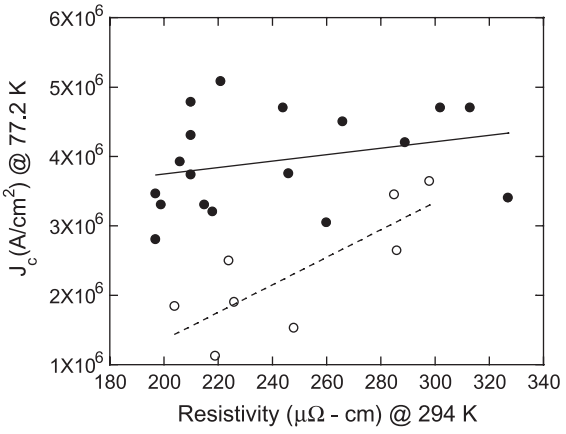

Fig. 8. Correlation of transport J_c and room temperature resistivity of films for films deposited at 120 mTorr (○) and 200–600 mTorr (●). Lines are linear fits with correlation coefficients $R = 0.80$ (○) and $R = 0.28$ (●).

1200 mTorr showed a high concentration of surface particulates, which may be related to the formation of YBCO nanoparticles in the vapor phase that can attach to the surface with low concentration and form nucleation centers for undesired growth [23].

The precise reason why T_c and J_c were decreased at lower O_2 pressures has not been fully answered yet. The oxygen content of the films as measured by XRD was constant for all O_2 deposition pressures. The average oxygen content was 6.96 ± 0.02, using the formula $X = 77.085 - 6.015 * D$ where X is the oxygen content and D is the average lattice spacing in Angstroms [24]. However, films deposited at different O_2 pressures showed distinct differences in impurity content. A film deposited at 120 mTorr had detectable (albeit minute) amounts of Al, Fe and Cr impurity in it as measured by SIMS, unlike one deposited at 600 mTorr. The increase in impurity content could presumably come from interaction (and sputtering) of the plume with the heater block and support structures (Fig. 1). The heater block did show evidence

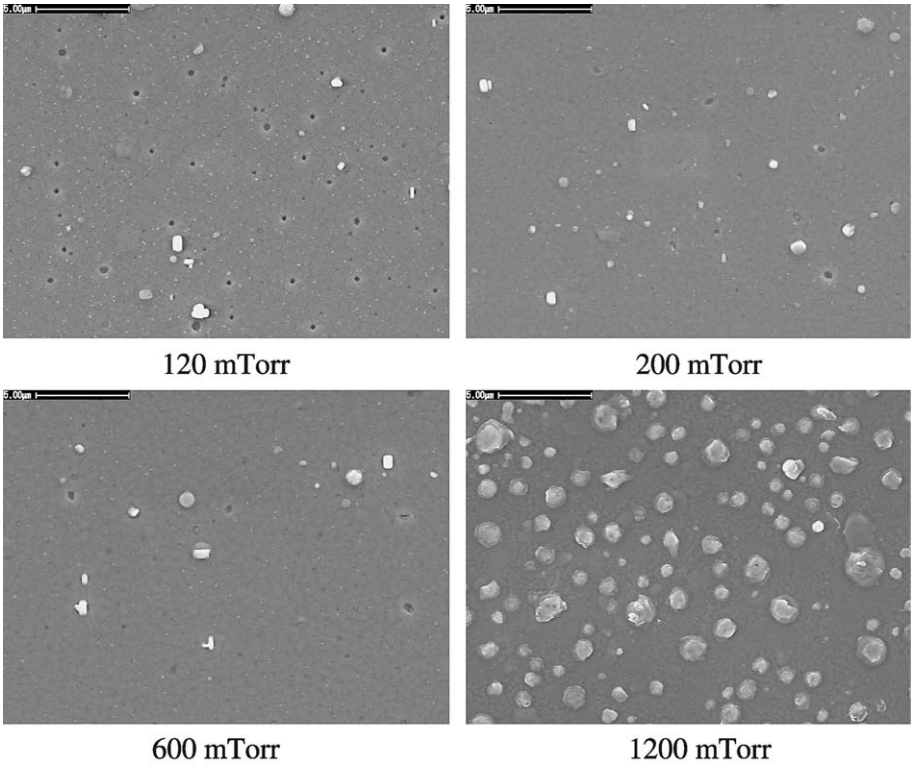

Fig. 9. SEM micrographs at 5000× magnification of YBCO film surfaces for varying O_2 deposition pressure.

of pitting indicating the potential interaction with the plume.

4. Discussion and proposed film growth mechanisms

Previously, the only model to describe the dependence of film growth on oxygen pressure was the so-called *P–D* model, where the sensitivity to oxygen pressure was proposed to be due to varying particle bombardment velocities; optimal film properties were only obtained by precisely varying either pressure (P) or distance (D) to achieve the particle velocity $\sim PD^{5(1-n)} = \text{const}$ where n is a constant in the range of 0.4–0.6 that fits the experimental *P–D* data [7]. For a fixed distance D, at less-than-ideal O_2 pressure the particle velocity was too high for optimal deposition, and at higher-than-ideal O_2 pressure the plume was shortened and the particle velocity was reduced below the value required for adequate surface activation.

Herein, the results are not consistent with this model and indicate that different mechanisms or models must be considered for film growth at higher temperatures. Optimized growth was achieved with the substrate located well within the plume ($D/L_p \sim 0.7$ at 200 mTorr) where particle velocities are typically very high $\sim 10^6$ cm/s, and also achieved outside the plume ($D/L_p \sim 1.2$ at 1200 mTorr) where particle velocities are ~thermalized [5]. To explain why these new results were achieved, two mechanisms are proposed as described following.

Mechanism (1): *At the higher substrate temperature of 785 °C, the surface activation is sufficient for film growth and not dependent on the additional mechanism of velocity bombardment*. This was proposed in Ref. [7] to reduce the sensitivity (however, not completely eliminate it), and helps explain why the results in Fig. 4 for ~780 °C substrate temperatures for Refs. [8–10] are not as sensitive as the curve at lower temperature of 680 °C from Ref. [7]. The range of temperatures required to obtain sufficient surface activation was not determined in this work. Preliminary studies found T_cs consistent with Fig. 4 when the heater block temperature was varied from 755 to 805 °C. A temperature of at least 700 °C was necessary to obtain T_cs > 80 K in one study [11].

Mechanism (2): *The particle velocity at the substrate must remain below a critical value, to prevent high velocity particle bombardment which results in degradation of T_c and J_c*. This supposition is consistent with the *P–D* model for less-than-ideal O_2 pressures. Optimum growth occurred herein for $D/L_p \sim 0.7$–1.2, and degradation was observed only for $D/L_p \sim 0.6$, when the substrate was located closer to the center of the plume. The velocity of the plume shock front decreases as it expands into partial O_2 pressure typically as expected from a simple Beer's law model of scattering $I = I_0 E^{-N\sigma x}$, where I is the integrated ion–probe current, N is the pressure, x is the distance and σ is the generalized cross-section $\sim 2 \times 10^{-16}$ cm^2 for ion oxygen collisions [5,25]. As the O_2 pressure is increased from 50 to ~300 mTorr, the plume experiences increased collisions and decreases in velocity for a given distance D from the target. The decrease of particle velocity is consistently observed, as measured by integrated ion–probe current drops, and for varying laser fluence by optical spectroscopy of time-of-flight (TOF) emission profiles and electronic temperatures [5,25,26]. Specifically for similar conditions as this work (3.0 J/cm^2 fluence and 248 nm irradiation), the average particle velocity decreased by ~60% as the O_2 pressure was increased from 100 to 200 mTorr for $D = 5$ cm [5,25]. We propose that for the plume and substrate conditions in this work ($D/L_p \sim 0.6$, 120 mTorr) the particle velocity exceeded a critical value, above which film degradation occurred.

An interesting subtlety exists for deposition at higher O_2 pressure; however, which should be considered to explain the results herein and differences with other studies in Figs. 4 and 5. For O_2 pressure ~ 600 mTorr and higher, the temperature and particle velocity inside the plume ($D/L_p \sim 0.4$–0.75) was observed to increase for fixed D positions, as the plume energy became increasingly restricted to a smaller region with higher O_2 pressure [26]. This velocity increase in the center region of the plume was easily observed from real-time camera imaging of the plume, especially for 1200 mTorr velocity, and was consistently measured for different laser fluence using TOF spectrums and thermal spectroscopy for varying laser fluence as the pressure was increased from ~600 to

1200 mTorr [26]. Therefore, we believe placement of the substrate in the plume is also an important contributing factor to give the non-sensitivity to O_2 pressure as shown herein. For higher pressures and unknown particle velocities, it is might be considered safest to position the substrate near or beyond the plume edge ($D/L_p > \sim 0.8$), where the particle velocity experiences a sharp gradient drop in temperature and velocity to reach thermal equilibrium beyond the plume edge ($D/L_p > 1.0$). These conditions were satisfied for the work herein. In contrast, if the substrate is placed near the center of the plume ($D/L_p \sim 0.5$), at higher pressures the substrate can be exposed to increasing particle velocities as the O_2 pressure is increased. This mechanism may explain why plots from Refs. [8–10] in Fig. 4 for ~780 °C substrate temperature have decreased T_c at higher-than-optimal O_2 pressure, in contrast with results from this work.

The role of laser fluence was not fully explored in this paper. With higher energy deposited E_0, the plume extends further and the particle velocities are higher inside the plume; for the blast wave model the shock front velocity $\sim$ const $*$ $(E_0/\rho_0)^{1/5}t^n$, where ρ_0 is the gas pressure, t is time, and n is a constant that models the distance versus time experimental data of the plume expansion front [5,25]. Therefore for higher fluences, one would expect that the substrate should be placed further towards the plume edge ($D/L_p > 0.6$ for our conditions) to avoid damaging particle velocities. Preliminary experiments varying the fluence to move the substrate location in the plume were consistent with this consideration and the mechanisms above. At 300 mTorr, the laser fluence was varied from 2.2 to 3.2 J/cm^2 ($D/L_p \sim 0.8$–1.0) by increasing the laser energy, and the T_cs and J_cs were not greatly affected. At 1200 mTorr, the plume was extended by changing the focusing optics to narrow the beam considerably ($D/L_p \sim 0.8$), or increasing the fluence to 4.5 J/cm^2 by increasing the laser energy ($D/L_p \sim 1.1$), and for both of these cases there was no effect on T_cs or J_cs (see Fig. 5 for higher fluence).

It should also be noted that in the work herein, the window of optimized deposition included a large region from 200 to 600 mTorr when the substrate was located inside the plume ($D/L_p \sim 0.7$–1.0). This result is in contrast with previous results, where films deposited at $D/L_p \sim 0.7$ contained very large and well-separated grains and lower J_c [12], and optimized results were obtained at the plume edge $D/L_p \sim 1.0$. We believe this is also a consequence of the optimized particle velocity for these O_2 pressures, as discussed above.

5. Conclusions

High quality YBCO films were deposited for a wide range of O_2 deposition pressure, with the substrate located both inside and outside of the plume ($D/L_p \sim 0.7$–1.2). T_cs > 91.5 K and excellent four-probe transport J_cs of 3–5 MA/cm^2 at 77 K in self-field, were consistently and reliably obtained for O_2 pressures from 200 to 1200 mTorr. The films always had a mirror-like surface finish when grown inside the plume (O_2 pressure $\leqslant$ 600 mTorr, $D/L_p \sim 0.6$–1.0). Room temperature resistivities, T_cs, J_cs and microstructures all had slightly varying dependence on O_2 pressure. The relative insensitivity to O_2 pressure is proposed to be a consequence of two mechanisms: (1) growth at 780 °C does not require additional surface activation from particle bombardment, and (2) the velocity of particle bombardment must be reduced below a critical threshold value to prevent degradation of film properties; for the conditions of this study the substrate was placed near-or-beyond the plume ($D/L_p > 0.7$). We believe this is the first report where T_cs at 92 K and J_cs from 3–5 MA/cm^2 have reliably and repeatably been obtained in YBCO thin films for a wide range of O_2 deposition pressures. The relative insensitivity of T_c and J_c to O_2 pressure for the conditions studied will provide useful information for any PLD optimization and scale-up.

Acknowledgements

The Air Force Office of Scientific Research supported this work. J.S. Solomon [Solomon James S Contr AFRL/MLPS] of the University of

Dayton Research Institute performed the SIMS analysis. The authors would like to thank R. Feenstra of Oak Ridge National Laboratory for valuable discussions on room temperature resistivity, and J. Evans, T. Spry and M.E. Fowler for assistance with thickness and critical current measurements.

References

[1] A. Bourdillon, N.X. Tan Bourdillon, High Temperature Superconductors: Processing and Science, Academic Press, San Diego, CA, 1994.
[2] Y. Iijima, K. Onabe, N. Tugaki, N. Tanabe, N. Sadakara, O. Kohno, Y. Ikeno, Appl. Phys. Lett. 60 (1992) 769.
[3] X.D. Wu, S.R. Foltyn, P.N. Arendt, W.R. Blumenthal, I.H. Campbell, J.D. Cotton, J.Y. Coulter, W.L. Hults, M.P. Maley, H.F. Safar, J.L. Smith, Appl. Phys. Lett. 67 (1995) 2397.
[4] A. Goyal, D.P. Norton, J.D. Budai, M. Paranthaman, E.D. Specht, D.M. Kroeger, D.K. Christen, Q. He, B. Saffian, F.A. List, D.F. Lee, P.M. Martin, C.E. Klabunde, E. Hartfield, V.K. Sikka, Appl. Phys. Lett. 69 (1996) 1795.
[5] D.B. Chrisey, G.K. Hubler (Eds.), Pulsed Laser Deposition of Thin Films, John Wiley and Sons, New York, NY, 1994.
[6] T. Morrow, H.F. Sakeek, A.S.l. Astal, W.G. Graham, D.G. Walmsley, J. Superconduct. 7 (1994) 828;
G. Perram et al., Air Force Institute of Technology, Private communication.
[7] H.S. Kim, H.S. Kwok, Appl. Phys. Lett. 61 (1992) 2234.
[8] E.H. Lee, S.J. Park, I. Hun Song, I. Song, J. Gohng, J. Sok, J.W. Lee, D.Y. Jeon, C.Y. Dosquet, IEEE Trans. Appl. Supercond. 7 (1997) 1193.
[9] S. Duhalde, A. Lamagna, M. Villafuerte, A. Schwartzman, L. Correra, G. Quintana, Appl. Surf. Sci. 127 (1998) 520.
[10] D.A. Rudman, F.J.B. Stork, J.C. Booth, J.Y. Juang, L.R. Vale, G.J. Beaty, C.I. Williams, J.A. Beall, R.H. Ono, S.B. Qadri, M.S. Osofsky, E.F. Skelton, J.H. Claassen, G. Gibson, J.L. MacManus-Driscoll, N. Malde, L.F. Cohen, IEEE Trans. Appl. Supercond. 9 (1999) 2460.
[11] H. Huhtinen, P. Paturi, E. Lahderanta, R. Laiho, Supercond. Sci. Technol. 12 (1999) 81.
[12] F. Goerke, A. Thorns, Physica C 251 (1995) 247.
[13] P.E. Dyer, A. Issa, P.H. Key, Appl. Surf. Sci. 46 (1990) 89.
[14] J. García López, D.H.A. Blank, H. Rogalla, Appl. Surf. Sci. 127 (1998) 1011.
[15] Superconductive Components Inc., 1145 Chesapeake Ave., Columbus, OH 43212.
[16] Neocera Inc., 10000 Virginia Manor Rd., Beltsville MD, 20705.
[17] J.W. Ekin, T.M. Larson, N.F. Bergren, A.J. Nelson, A.B. Swartzlander, L.L. Kazmerski, A.J. Panson, B.A. Blankenship, Appl. Phys. Lett. 52 (1988) 1819.
[18] L.F. Goodrich, A.N. Srivastava, T.C. Stauffer, A. Roshko, L.R. Vale, IEEE Trans. Appl. Supercond. 4 (1994) 61.
[19] I. Maartense, A.K. Sarkar, G. Kozlowski, Physica C 181 (1991) 25.
[20] A. Sarkar, B. Kumar, I. Maartense, T.L. Peterson, J. Appl. Phys. 65 (1989) 2392.
[21] G.V.M. Williams, J.L. Tallon, Physica C 258 (1996) 41.
[22] S.K. Hau, K.H. Wong, P.W. Chang, C.L. Choy, Appl. Phys. Lett. 66 (1995) 245.
[23] P.N. Barnes, P.T. Murray, T. Haugan, R. Rogow, G.P. Perram, Physica C 377 (2002) 578.
[24] H.Y. Zhai, Z.H. Zhang, W.K. Chu, in: Paper presented at ASC 2002 Conference, Houston, TX.
[25] B. Geohegan, in: J.C. Miller, R.F. Haglund (Eds.), Laser Ablation: Mechanisms and Applications, Springer-Verlag, Heideberg, 1991, p. 28.
[26] G. Perram et al., in: Paper presented at the March 2002 American Physical Society Meeting.